

Role of isospin in the nuclear liquid-gas phase transition

C. Ducoin^(1,2), Ph. Chomaz⁽¹⁾ and F. Gulminelli⁽²⁾

(1) *GANIL (DSM-CEA/IN2P3-CNRS), B.P.5027, F-14076 Caen cédex 5, France*

(2) *LPC (IN2P3-CNRS/Ensicaen et Université), F-14050 Caen cédex, France*

We study the thermodynamics of asymmetric nuclear matter using a mean-field approximation with a Skyrme effective interaction, in order to establish its phase diagram and more particularly the influence of isospin on the order of the transition. A new statistical method is introduced to study the thermodynamics of a multifluid system, keeping only one density fixed, the others being replaced by their intensive conjugated variables. In this ensemble, phase coexistence reduces to a simple one-dimensional Maxwell construction. For a fixed temperature under a critical value, a coexistence line is obtained in the plane of neutron and proton chemical potentials. Along this line, the grand potential presents a discontinuous slope, showing that the transition is first order except at the two ending points where it becomes second order. This result is not in contradiction with the already reported occurrence of a continuous transformation when a constant proton fraction is imposed. Indeed, the proton fraction being an order parameter in asymmetric matter, the constraint can only be fulfilled by gradual phase mixing along the first-order phase-transition line, leading to a continuous pressure.

PACS numbers: 24.10.Pa,64.60.Fr,68.35.Rh

I. INTRODUCTION

Nucleons in atomic nuclei interact through a finite-range attractive and a short-range repulsive force. For systems of particles interacting this way, one expects to find a phase transition analogous to the liquid-gas transition of a van der Waals fluid [1]. As a matter of fact, it is recognized that symmetric nuclear matter should undergo a first-order transition between a low (gas) and a high (liquid) density phase up to a critical temperature [2, 3, 4]. For such a system containing an equal number of neutrons and protons, isospin symmetry imposes that the nucleons behave as one single fluid and one expects a discontinuous density versus pressure equation of state.

The case of asymmetric matter is more complex to study, since there is an additional degree of freedom to consider: the isospin. Such matter plays an important role in astrophysics, where neutron-rich systems are involved in neutron stars and type-II supernova evolution [5, 6]. For asymmetric systems containing a fixed proton fraction, it has been shown that the thermodynamic transformations result in a continuous evolution of the observables. In particular, the system density is a continuous function of the pressure. This has been interpreted as the occurrence of a continuous transition [7, 8, 9, 10, 11, 12]. We will show in the present article that this conclusion is not correct: it results from a confusion between the notions of 'continuous transition' and 'continuous transformation'. Indeed, the phenomenon of isospin distillation demonstrates that the proton fraction is an order parameter in asymmetric nuclear matter. Thus, when the proton fraction is kept constant, the system is forced to follow the first-order phase-transition line, hiding the discontinuity of the thermodynamic potential first derivative.

The plan of the paper is as follows: we calculate in Section II the nuclear matter grand potential in the

mean-field approximation using a Skyrme (Sly230a) energy density functional [13]. The thermodynamics of nuclear matter has been addressed earlier with different effective forces [15, 16, 17, 18]. The construction of phase coexistence is presented in section III. It consists in correcting the mean-field instabilities with the introduction of phase separation, in order to build the concave envelope of the thermodynamic potential. To perform this Gibbs construction with an arbitrary number of conserved quantities, we introduce a new method that reduces this multidimensional problem to a simple one-dimensional Maxwell construction on a carefully defined statistical potential. The results of this analysis are presented in section IV. The grand-canonical potential presents a discontinuous derivative on both sides of a bi-dimensional manifold limited by a critical line in the 3-dimensional space including the temperature and the proton and neutron chemical potentials. The transition is thus first order for all associated proton fractions. Only the critical line corresponds to continuous transitions. An interesting point is that in this 3-dimensional problem the critical line can be characterized by additional critical exponents as the chemical potential approaches its critical value for a given temperature. We first present the coexistence region obtained for a fixed temperature, stressing the isospin properties of phase coexistence. Then, the thermodynamic consequences of a transformation at constant proton fraction are analyzed. We show that this transformation forces the system to follow the coexistence line, and this is the generic behavior expected when a conservation law acts on an order parameter. In this case, the first-order phase transition results in a continuous transformation from a diluted to a dense system through a phase coexistence, which should not be confused with a continuous transition. Indeed, one should clearly make the difference between a transformation, which is a specific path in the space of ther-

mododynamic variables, and a phase transition which is an anomaly of the thermodynamic potential considered in the total space of thermodynamic variables [28]. The temperature dependence of the phase diagram is finally explored, and the critical behaviour is presented.

II. THERMODYNAMICS WITH SKYRME FORCES

A. Isospin dependent energy functional

We study the case of nuclear matter in a mean-field approach, with the SLy230a Skyrme effective interaction [13]. This local interaction allows to introduce an energy density $\mathcal{H}(\mathbf{r})$ so that the total energy for a system of nucleons in a Slater determinant $|\psi\rangle$ reads :

$$\langle\psi|\hat{H}|\psi\rangle = \int \mathcal{H}(\mathbf{r}) d\mathbf{r} \quad (1)$$

where \hat{H} is the Hamiltonian of the system. The energy density \mathcal{H} is a functional of the particle densities ρ_q and kinetic densities τ_q for neutrons ($q = n$) and protons ($q = p$). Denoting $\hat{\rho}_q$ the one-body density matrix of the particles of type q , those quantities are expressed as follows: $\rho_q(r) = \langle r|\hat{\rho}_q|r\rangle$ and $\tau_q(r) = \langle r|\frac{1}{\hbar^2}\hat{p}\hat{\rho}_q\hat{p}|r\rangle$, such that $\frac{\hbar^2}{2m}\tau_q$ is the kinetic energy density.

For later convenience it is useful to introduce the isoscalar and isovector densities :

$$\begin{aligned} \rho &= \rho_n + \rho_p, & \tau &= \tau_n + \tau_p \\ \rho_3 &= \rho_n - \rho_p, & \tau_3 &= \tau_n - \tau_p \end{aligned} \quad (2)$$

In the case of homogeneous, spin-saturated matter with no coulomb interaction, four terms contribute to the energy density :

$$\mathcal{H} = \mathcal{K} + \mathcal{H}_0 + \mathcal{H}_3 + \mathcal{H}_{eff} \quad (3)$$

In this expression, \mathcal{K} is the kinetic-energy term, \mathcal{H}_0 a density-independent two-body term, \mathcal{H}_3 a density-dependent term, and \mathcal{H}_{eff} a momentum-dependent term:

$$\mathcal{K} = \frac{\hbar^2}{2m}\tau \quad (4)$$

$$\mathcal{H}_0 = C_0\rho^2 + D_0\rho_3^2 \quad (5)$$

$$\mathcal{H}_3 = C_3\rho^{\sigma+2} + D_3\rho^{\sigma}\rho_3^2 \quad (6)$$

$$\mathcal{H}_{eff} = C_{eff}\rho\tau + D_{eff}\rho_3\tau_3 \quad (7)$$

The coefficients C_i and D_i , associated respectively with the symmetry and asymmetry contributions, are linear combinations of the traditional Skyrme parameters :

$$\begin{aligned} C_0 &= 3t_0/8 \\ D_0 &= -t_0(2x_0 + 1)/8 \\ C_3 &= t_3/16 \\ D_3 &= -t_3(2x_3 + 1)/48 \\ C_{eff} &= [3t_1 + t_2(4x_2 + 5)]/16 \\ D_{eff} &= [t_2(2x_2 + 1) - t_1(2x_1 + 1)]/16 \end{aligned} \quad (8)$$

To illustrate the SLy energy functional we present in figure 1 the energy density and the energy per particle as a function of the total particle density for various proton fractions. The kinetic-energy term has been computed integrating over the Fermi spheres associated with the considered proton and neutron densities. The minimum of the energy per particle is the saturation point of symmetric matter $\rho_0 = 0.16 \text{ fm}^{-3}$ and $E_0 = -15.99 \text{ MeV}$, while the curvature gives the incompressibility $K = 230.9 \text{ MeV}$. The $Z/A = 0$ curves correspond to pure neutron matter which does not saturate, the Sly forces being fitted on realistic neutron-matter EOS calculations [13, 18].

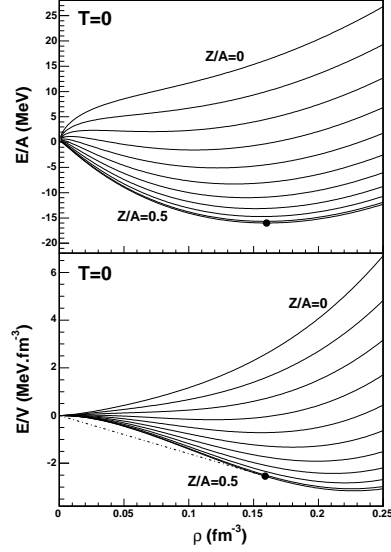


FIG. 1: Sly230a functional for infinite nuclear matter : energy per particle (upper part) and energy density (lower part) as functions of the total nucleon density for regularly spaced proton fractions from $Z/A=0.5$ to $Z/A=0$, in steps of 0.05.

The mean-field effective Hamiltonian \hat{W}_q for each particle-type q is defined by the relation $\delta\langle\hat{H}\rangle = Tr(\hat{W}_q\delta\hat{\rho}_q)$ i.e. as a functional derivative of the energy density. In the case of Skyrme interactions, this leads to the expression :

$$\hat{W}_q = \frac{\partial\mathcal{H}}{\partial\tau_q}\frac{\hat{p}^2}{\hbar^2} + \frac{\partial\mathcal{H}}{\partial\rho_q} = \frac{1}{2m_q^*}\hat{p}^2 + U_q \quad (9)$$

where $U_q = \partial_{\rho_q}\mathcal{H}$ is the local mean-field potential :

$$\begin{aligned} U_q &= U_{0_q} + U_{3_q} + U_{eff_q} \\ &= [2C_0\rho + (\sigma + 2)C_3\rho^{\sigma+1} + \sigma D_3\rho^{\sigma-1}\rho_3^2 + C_{eff}\tau] \\ &\quad \pm [2D_0\rho_3 + 2D_3\rho^{\sigma}\rho_3 + D_{eff}\tau_3] \end{aligned} \quad (10)$$

and the effective mass m_q^* is defined by :

$$\frac{\hbar^2}{2m_q^*} = \frac{\hbar^2}{2m} + C_{eff}\rho \pm D_{eff}\rho_3 \quad (11)$$

In both expressions, the \pm sign refers to neutrons (+) or protons (-).

In uniform nuclear matter, the eigenstates of this mean-field Hamiltonian are spin-up or spin-down plane waves with momenta \mathbf{p}_i . The single-particle energies are given by :

$$\epsilon_q^i = \frac{p_i^2}{2m_q^*} + U_q \quad (12)$$

B. Finite temperature

Within a mean-field approach, thermodynamic relations are easy to derive in the grand-canonical ensemble. For a system of neutrons and protons, the grand-canonical constraint imposes the average value of three observables: energy, number of protons and neutrons. Maximizing the Shannon entropy with these three constraints leads to an equilibrium partition sum :

$$Z_{GC} = \text{Tr}[e^{-\beta\hat{H} + \alpha_n\hat{N}_n + \alpha_p\hat{N}_p}] \quad (13)$$

where the inverse temperature $\beta = 1/kT$ is the Lagrange multiplier associated with the energy constraint, and $\alpha_q = \beta\mu_q$ are the Lagrange multipliers controlling the particle numbers $\langle \hat{N}_q \rangle$, μ_q being the chemical potentials. The Lagrange parameters fulfill the equations of state :

$$\langle \hat{H} \rangle = -\partial_\beta \ln Z_{GC} \quad (14)$$

$$\langle \hat{N}_q \rangle = \partial_{\alpha_q} \ln Z_{GC} \quad (15)$$

The self-consistent mean-field approximation amounts to use independent particle states as trial density matrices in the maximum-entropy variational principle: the single-particle states of energy ϵ_q^i are then occupied according to the Fermi-Dirac distribution [19] :

$$n_q^i = \frac{1}{1 + \exp(\beta(\epsilon_q^i - \mu_q))} \quad (16)$$

In infinite matter, n_q^i is a continuous distribution $n_q(p)$ and the densities ρ_q and τ_q read :

$$\rho_q = 2 \int_0^\infty n_q(p) \frac{4\pi p^2}{h^3} dp \quad (17)$$

$$\tau_q = 2 \int_0^\infty \frac{p^2}{h^2} n_q(p) \frac{4\pi p^2}{h^3} dp \quad (18)$$

where the factor 2 come from the spin degeneracy.

The first equation establishes a self-consistent relation between the density of q-particles ρ_q and their chemical potential μ_q . The above densities can be written as regular Fermi integrals by shifting the chemical potential according to $\mu'_q = \mu_q - U_q$. The Fermi-Dirac distribution indeed reads :

$$n_q(p) = \frac{1}{1 + \exp(\beta(p^2/2m_q^* - \mu'_q))} \quad (19)$$

Equations (19) and (17) define a self-consistent problem since m_q^* depends on the densities according to eq.(11). For each pair (μ'_q, μ'_p) a unique solution (ρ_n, ρ_p) is found by iteratively solving the self-consistency between $\rho_{n,p}$ and $m_{n,p}^*$. Then eq.(18) is used to calculate $\tau_{n,p}$. These quantities allow to compute the one-body partition sum :

$$Z_0 = \text{Tr}[e^{-\beta(\hat{W}_n + \hat{W}_p - \mu_n\hat{N}_n - \mu_p\hat{N}_p)}] = Z_0^n Z_0^p \quad (20)$$

where each partition sum Z_0^q can be expressed as a function of the corresponding kinetic energy density :

$$\frac{\ln Z_0^q}{V} = 2 \int_0^\infty \ln(1 + e^{-\beta(\frac{p^2}{2m_q^*} - \mu'_q)}) \frac{4\pi p^2}{h^3} dp = \frac{\hbar^2}{3m_q^*} \beta \tau_q \quad (21)$$

At the thermodynamic limit, the system volume V diverges together with the particle numbers $\langle \hat{N}_q \rangle$, and the thermodynamics is completely defined as a function of the two particle densities ρ_n, ρ_p .

We can now use the maximum-entropy variational principle to evaluate the mean-field approximation to the grand-canonical partition sum Z_{GC} . We recall that the exact grand-canonical ensemble corresponds to the maximum of the constrained Shannon entropy which is nothing but $\ln Z_{GC}$:

$$\ln Z_{GC} = S_{GC} - \beta(\langle \hat{H} \rangle_{GC} - \mu_n \langle \hat{N}_n \rangle_{GC} - \mu_p \langle \hat{N}_p \rangle_{GC}). \quad (22)$$

The variational principle thus states that the mean-field constrained entropy is the best approximation within the ensemble of independent-particle trial states to the exact maximum $\ln Z_{GC}$:

$$\ln Z_{GC} \simeq S_0 - \beta(\langle \hat{H} \rangle_0 - \mu_n \langle \hat{N}_n \rangle_0 - \mu_p \langle \hat{N}_p \rangle_0), \quad (23)$$

where the mean-field energy and particle numbers are defined as functions of densities, i.e. single-particle occupations eq.(19), by :

$$\langle \hat{H} \rangle_0 = V\mathcal{H}; \langle \hat{N}_q \rangle_0 = V\rho_q \quad (24)$$

The mean-field entropy is given by :

$$S_0 = \ln Z_0 + \beta(\langle \hat{W} \rangle_0 - \mu_n \langle \hat{N} \rangle_0 - \mu_p \langle \hat{N} \rangle_0) \quad (25)$$

where $\langle \hat{W} \rangle_0$ is the average single-particle energy :

$$\langle \hat{W} \rangle_0 = 2V \sum_q \int_0^\infty n_q(p) e_q(p) \frac{4\pi p^2}{h^3} dp = -\partial_\beta \ln Z_0 \quad (26)$$

with $e_q(p) = p^2/2m_q^* + U_q$.

The grand-canonical partition sum in the mean-field approximation is thus modified with respect to the independent-particle partition sum Z_0 as :

$$\ln Z_{GC} \simeq \ln Z_0 + \beta \left(\langle \hat{W} \rangle_0 - \langle \hat{H} \rangle_0 \right) \quad (27)$$

which allows to express the grand-canonical potential density as a function of densities :

$$-g = \frac{\ln Z_{GC}}{\beta V} \simeq \frac{2}{3}\mathcal{K} + \mathcal{H}_0 + (\sigma + 1)\mathcal{H}_3 + \frac{5}{3}\mathcal{H}_{eff} \quad (28)$$

At the thermodynamic limit, this quantity is equivalent to the system pressure $P = -g$. Because of ensemble equivalence we can then evaluate all the thermodynamic potentials. For example, the canonical partition sum, or equivalently the free energy per unit volume f , is defined through the Legendre transform :

$$f = -\frac{\ln Z_C}{\beta V} = g + \mu_n \rho_n + \mu_p \rho_p \quad (29)$$

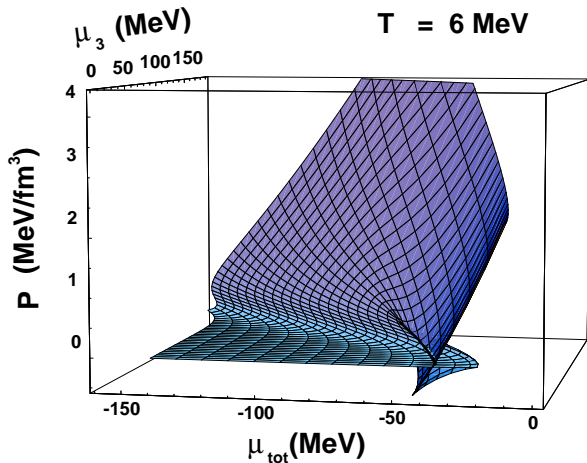


FIG. 2: Pressure as a function of the isoscalar and isovector chemical potentials for a uniform system at $T = 6\text{ MeV}$.

Figure 2 illustrates the typical behavior of the pressure as a function of the isoscalar and isovector chemical potentials $\mu = \mu_n + \mu_p$ and $\mu_3 = \mu_n - \mu_p$. This figure is computed for a uniform system at a fixed temperature. For symmetry reasons only the positive μ_3 are shown. We can see that for some values of (μ, μ_3) , there are three solutions corresponding to different values for the conjugated observables (ρ, ρ_3) . This is the phase-transition region. The true equilibrium is the solution minimizing the grand potential i.e. maximizing the pressure. Thus only the upper part of the pressure manifold corresponds to a thermodynamic equilibrium. At the resulting fold, the slope changes discontinuously, i.e. using $\rho_q = \partial g / \partial \mu_q$, the equilibrium uniform system jumps from a low to a high density solution. It is a liquid-gas first-order phase transition. The fold of the grand potential is more clearly shown in figure 3 which presents the pressure as a function of μ_p for different values of μ_n .

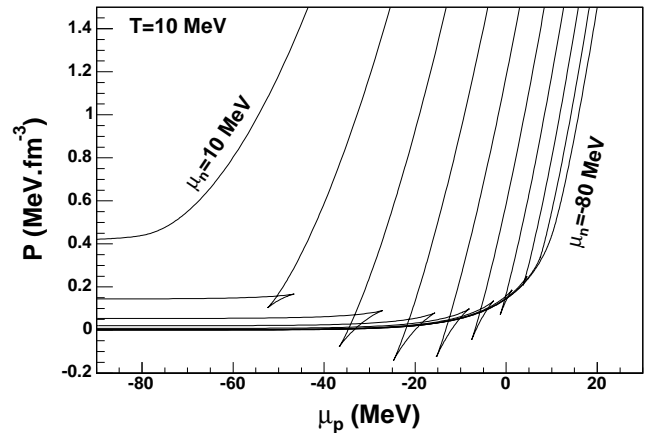


FIG. 3: Pressure as a function of μ_p for a uniform system at a fixed temperature $T = 10\text{ MeV}$ and regularly spaced values of μ_n from -80 to 10 MeV.

III. PHASE COEXISTENCE

A. Phase-coexistence conditions in multi-fluid systems

For systems at the thermodynamic limit, the existence and the order of a phase transition are intrinsically related to the singularities of the thermodynamic potential, $-T \ln Z(\lambda)$ where $Z(\lambda)$ is the partition sum for a given macroscopic state characterized by the L intensive parameters $\lambda = \{\lambda_\ell\}$ [14]. These intensive parameters are the Lagrange multipliers introduced in the maximization of the Shannon entropy under the L constraints $\langle \hat{A}_\ell \rangle$ associated with all the L relevant observables \hat{A}_ℓ .

A system presents a first-order phase transition if one of the first partial-derivatives of $\ln Z(\lambda)$ shows a discontinuity [1]. If a non-analyticity (discontinuity or divergence) is present at a higher order derivative, there is a continuous transition. Since the equations of states (EOS) are the L relations $\langle \hat{A}_\ell \rangle(\lambda) = -\partial_{\lambda_\ell} \ln Z(\lambda)$ [14], we can see that a first-order phase transition corresponds to a discontinuity in at least one of the EOS, i.e. to a jump in the mean value of at least one observable at the transition point. This observable can then be identified with an order parameter, since its value allows to distinguish the two coexisting phases.

At the thermodynamic limit, the entropy S , as all the extensive variables $\{A_k\}$, is additive and thus scales like the volume V :

$$S(V, \{A_k\}) = V s(\rho_k = \{A_k/V\}) \quad (30)$$

The volume can thus be eliminated from the thermodynamic description while the other extensive variables can be expressed as densities $\rho = \{\rho_k\}$. If we consider two isolated systems of volume $V_1 = \alpha V$ and $V_2 = (1 - \alpha)V$, their constrained entropy is simply the sum of the two en-

tropies $S = S_1 + S_2$. When 1 and 2 are put into contact to form a system with $\rho = \alpha\rho_1 + (1 - \alpha)\rho_2$, equilibrium is reached by maximization of the global entropy S so that :

$$S \geq S_1 + S_2. \quad (31)$$

This imposes the convexity of the entropy :

$$s(\alpha\rho_1 + (1 - \alpha)\rho_2) \geq \alpha s(\rho_1) + (1 - \alpha)s(\rho_2) \quad (32)$$

As a result, if the homogeneous system has a constrained entropy with a convex region, a linear interpolation between two densities ρ_A and ρ_B corresponds to a physical phase mixing of the two associated states. Such linear interpolations lead to the construction of a concave envelope which maximizes the entropy functional and suppresses the curvature anomaly (Gibbs construction). The straight lines corresponding to phase coexistence are defined by two points of same tangent plane, i.e. with identical first derivatives or intensive variables $\lambda_k = \partial_{\rho_k} s$, and equal values of the constrained entropy, i.e. equal distances between the entropy $s(\rho)$ and the plane $\sum_k \lambda_k \rho_k = 0$. Using $[\partial_V S(V, \{A_k\})]/V = s(\{\rho_k\}) - \sum_k \lambda_k \rho_k$ this latter condition can be interpreted as the equality of the two system pressures. This equality of all intensive variables defines the conditions of phase equilibrium.

B. Gibbs and Maxwell constructions

For nuclear matter at a given temperature, the A_k are the proton and neutron numbers: $N = \rho_n V$ and $Z = \rho_p V$. Finding two points in equilibrium means finding two sets of densities $\{\rho_n^A, \rho_p^A\}$ and $\{\rho_n^B, \rho_p^B\}$ which fulfill the 3 equations $\mu_n^A = \mu_n^B$, $\mu_p^A = \mu_p^B$, $P^A = P^B$, the equality of the temperatures being insured by the use of an isothermal ensemble. The path corresponding to a constant μ_q (e.g. μ_n) is a curve in the (μ_p, P) plane that can be determined numerically. The problem is now reduced to two dimensions: if this path shows a crossing point, there are two sets of extensive observables for which the intensive parameters are all equal, which is the condition for coexistence. This is illustrated in the central part of figure 4.

From the thermostatistics point of view, using the set of state variables (β, μ_n, ρ_p) corresponds to defining a neutron-grand-canonical but proton-canonical ensemble, denoted as pC in the following. The associated potential per unit volume, $G_{pC}/V = g_{pC}$, is given by :

$$g_{pC}(\beta, \mu_n, \rho_p) = \mathcal{H} - \mu_n \rho_n - s(\mathcal{H}, \rho_n, \rho_p)/\beta \quad (33)$$

where $s = S/V$ is the entropy density. g_{pC} is linked by Legendre transforms both to the grand-canonical potential $g_{GC} = -P$ (pressure) and to the canonical potential f (free energy) :

$$g_{pC} = -P + \mu_p \rho_p = f - \mu_n \rho_n. \quad (34)$$

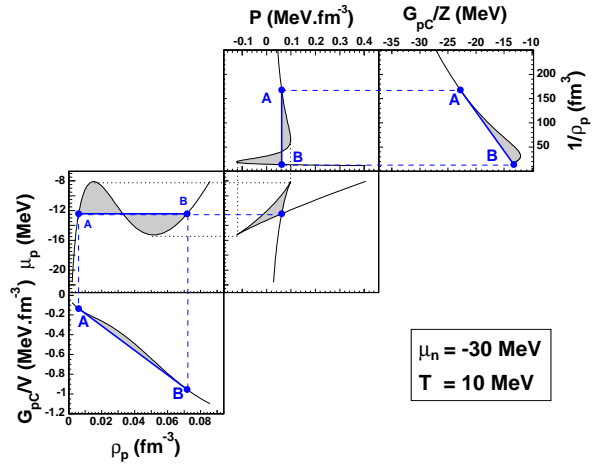


FIG. 4: Illustration of a Maxwell-Gibbs construction in the proton-canonical and neutron-grand-canonical ensemble at a fixed neutron chemical potential $\mu_n = -30\text{ MeV}$ and temperature $T = 10\text{ MeV}$. The bottom part presents the thermodynamic potential density G_{pC}/V as a function of the proton density ρ_p . The straight line shows the convex envelop interpolating between the two phases A and B . This corresponds to the Maxwell construction on μ_p as a function of ρ_p (left center). The top-right part shows the convex envelop of the thermodynamic potential per particle G_{pC}/Z as a function of the inverse of the proton density $1/\rho_p$ which is associated with a Maxwell construction for the pressure as a function of $1/\rho_p$ (top center). The two Maxwell constructions correspond to the crossing of the P - μ_p diagram (central figure).

It is important to stress that ensembles are equivalent at the thermodynamic limit which is used in the presented mean-field approach. The difference comes from the thermodynamical variables and potentials that are used. Therefore, the construction of the phase transition is not the same. The proposed ensemble leads to a simple 1-dimensional Maxwell construction which is much simpler than the usual multidimensional Gibbs construction in a multi-fluid system. Namely, for the considered system:

- In the canonical ensemble, the variables are the densities (ρ_n and ρ_p) and the potential is the free energy f . The Gibbs construction is then a complex 2-dimensional construction of its convex envelope.
- In the grand-canonical ensemble, the variables are the chemical potentials (μ_n and μ_p) and the potential is the grand potential g . In a first-order phase-transition region this function is multivalued. The Gibbs construction is then a complex 2-dimensional construction of the intersection of two of the three manifolds.
- In the proposed ensemble, the variables are one density (e.g. ρ_p) and one chemical potential (μ_n) and the potential g_{pC} is the corresponding Legendre transform of f and P . Since this ensemble has

only one density left, the phase coexistence is reduced to a simple problem like in a 1-component fluid. At constant μ_n , g_{pC} as a function of ρ_p should be replaced by its convex envelope. This is now a 1-dimensional problem which is in fact the usual Maxwell construction.

Numerically, we can directly perform this Maxwell construction on the function $\mu_p(\rho_p)$ for constant β and μ_n . The comparison between the results obtained using this method and the method described in the previous section using the $\mu_p - P$ crossing point gives an estimation of our numerical error, which comes out to be less than 0.2% for all temperatures.

We can additionally remark that the above reasoning also holds if we study the pC -potential per proton leading to a Maxwell construction for the pressure P as a function $1/\rho_p$. Both constructions are illustrated on figure 4. The convex envelop of G_{pC}/V (G_{pC}/Z) corresponds to an equal-area Maxwell construction on $\mu_p(\rho_p)$ ($P(1/\rho_p)$) and to the crossing point between the two phases in the μ_p versus P graph.

It should be noticed that the introduction of a statistical ensemble in which only one density is kept, all the other ones being replaced by their associated intensive parameters, can always be applied to study a phase transition with a one-dimensional order parameter. The only condition is that the considered density is not orthogonal to the order parameter, i.e. its value is different in the two phases. In such an ensemble, the multidimensional Gibbs construction reduces to a simple one-dimensional Maxwell construction.

IV. RESULTS

A. Coexistence region

In order to explore the phase diagram, the method illustrated in the previous section has to be performed for various temperatures and chemical potentials. Figure 5 illustrates the μ_n dependence for $T = 10$ MeV. We can see that for a broad range of μ_n the $\mu_p(\rho_p)$ equations of state present a back-bending associated with an instability which must be corrected using a Maxwell construction. This defines the transition points $\mu_p^t(\mu_n, T)$ and $P^t(\mu_n, T)$. The ensemble of the transition points constitutes a coexistence curve at the considered temperature. This curve is limited by two critical chemical potentials, $\mu_n^<(T)$ and $\mu_n^>(T)$, which in turn define the proton critical chemical potentials $\mu_p^>(T) = \mu_p^t(\mu_n^<(T), T)$ and $\mu_p^<(T) = \mu_p^t(\mu_n^>(T), T)$, since μ_p is maximum when μ_n is minimum. The transition is observed only in a finite range of temperatures below a given temperature T_c which is nothing but the critical temperature of symmetric matter.

The Gibbs construction of phase coexistence leads to well defined partition sums fulfilling the thermodynamic stability requirement. The resulting pressure $P =$

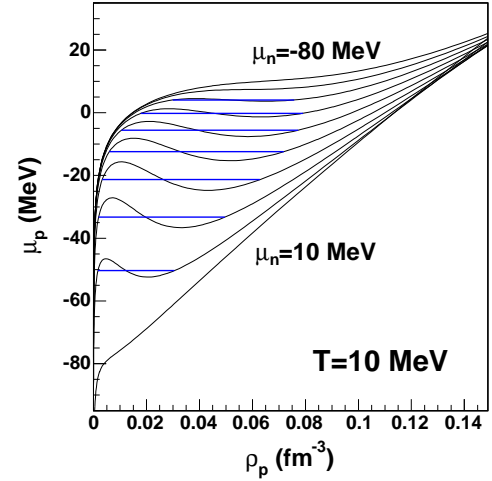


FIG. 5: Maxwell construction in the μ_p versus ρ_p diagram for a fixed temperature $T = 10$ MeV and regularly spaced values of μ_n from -80 to 10 MeV.

$T \ln Z_{GC}(T, \mu_n, \mu_p)/V$ at the temperature $T = 10$ MeV is shown in figure 6.

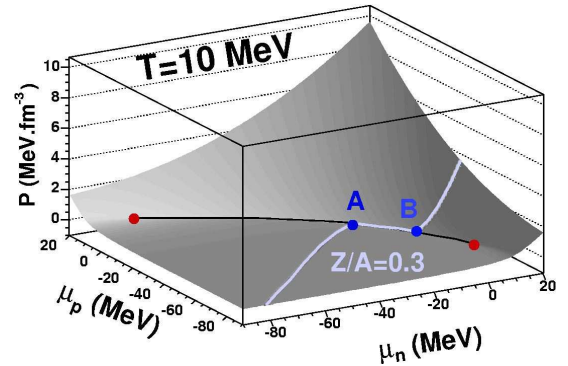


FIG. 6: Equilibrium pressure computed at a temperature $T = 10$ MeV as a function of μ_n and μ_p after performing a Gibbs construction for different values of μ_n . The resulting fold line is the coexistence line ending at two critical points. The traced path corresponds to a transformation at constant proton fraction $Z/A = 0.3$ (see Section IV-B).

Along the coexistence line $\mu_p^t(\mu_n, T)$, the pressure presents a fold, i.e. the derivative perpendicular to the line is discontinuous. It is by definition a region of first-order phase transition. The coexistence line at fixed temperature is limited by two points $(\mu_n^<(T), \mu_p^>(T))$ and $(\mu_n^>(T), \mu_p^<(T))$. They correspond to vertical tangents in the grand-potential first derivatives $\rho_q(\mu_n, \mu_p)$, which are singularities in its second derivatives. Hence, the limiting points are second-order critical points, i.e. points of continuous transition.

We have represented in figure 7 the first derivative of $\ln Z_{GC}$ in the μ_n direction, i.e. the neutron density

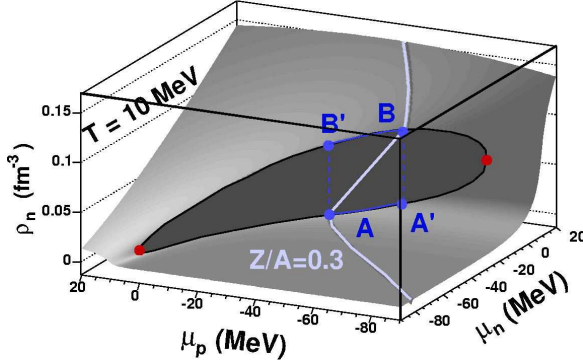


FIG. 7: First derivative of the grand-canonical partition sum, $\rho_n = \partial p / \partial \mu_n$, as a function of μ_n and μ_p at a temperature $T = 10 \text{ MeV}$. The path $Z/A = 0.3$ is also shown.

$\rho_n = \partial_{\mu_n} p$, which is discontinuous on the first-order line and continuous with a vertical tangent at the two critical points. Because of the exact isospin symmetry of the SLy interaction, the proton density ρ_p is symmetric to ρ_n : it is the same surface with inversion of the axes μ_n and μ_p .

The first derivatives of $\ln Z_{GC}$ on both sides of the phase transition line define pairs of points (ρ_n, ρ_p) in coexistence respectively at low (gas) and high (liquid) density. These phases merge together at the critical points. The coexistence region in the proton and neutron-density space is shown on figure 8 for a fixed temperature. The solid lines in this figure give several iso- μ_n paths. Because the construction of the concave envelop of the constrained entropy is nothing but a linear interpolation between two phases, inside the coexistence region the iso- μ_n lines are straight lines in (ρ_n, ρ_p) representation. The bottom part of the figure shows the coexistence region in the total-density and proton-fraction plane $(\rho, Z/A)$, which consists in the change of variables $\rho = \rho_n + \rho_p$, $y = Z/A = \rho_p / (\rho_n + \rho_p)$. Because of the non-linearity of the variable change, we can see that coexistence does not correspond to a straight line in this representation, and the value of Z/A evolves when passing from the dense phase to the diluted phase in coexistence. The only exception is the case of symmetric nuclear matter, at $y = Z/A = 0.5$.

The proton-fraction difference in the two phases can be appreciated from figure 9 which shows Z/A as a function of μ_n and μ_p for a fixed temperature $T = 10 \text{ MeV}$. Z/A being a combination of the two order parameters ρ_n and ρ_p , it also presents a discontinuity at the first-order phase-transition border, with the only exception of the symmetric nuclear matter point where $Z/A = cst = 0.5$. Correlating this plot with figure 7, one can see that the dense phase (e.g. point B' or B) is systematically closer to isospin symmetry $Z/A = 0.5$ than the diluted one (e.g. point A or A'). This phenomenon is known as isospin distillation [7, 20, 21].

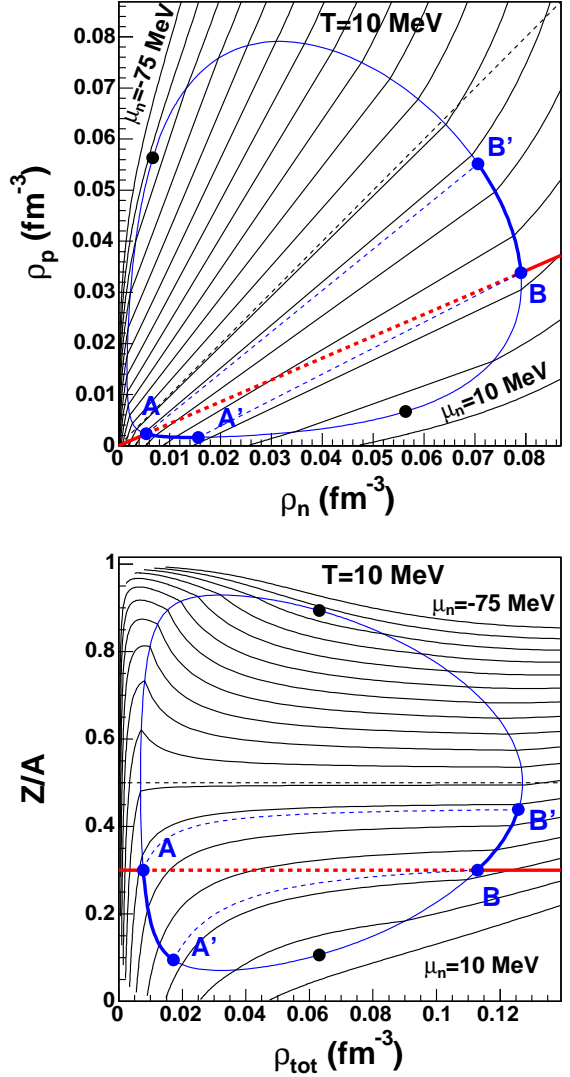


FIG. 8: Closed curves : coexistence border in the proton and neutron-density plane (upper part) and total-density and proton-fraction plane (lower part). Black dots : critical points. Full lines : constant μ_n paths for regularly spaced values between $\mu_n = 10 \text{ MeV}$ and -75 MeV . Paths AA' and BB' refer to a transformation at $Z/A = 0.3$ (see Section IV-B).

B. Transformation at constant Z/A

In low-energy heavy-ion collisions, the proton and neutron numbers obey two independent conservation laws, implying that the proton fraction Z/A is conserved in the reaction. It is therefore of interest to consider a transformation at constant Z/A [7, 21]. In the (ρ_n, ρ_p) plane (or equivalently in the $(\rho_{tot}, Z/A)$ representation) $Z/A = cst$ transformations are straight lines which cross the different constant- μ_n curves. Inside the coexistence region, the system with a given proton fraction is decomposed into two phases, located at the intersections of the coexistence

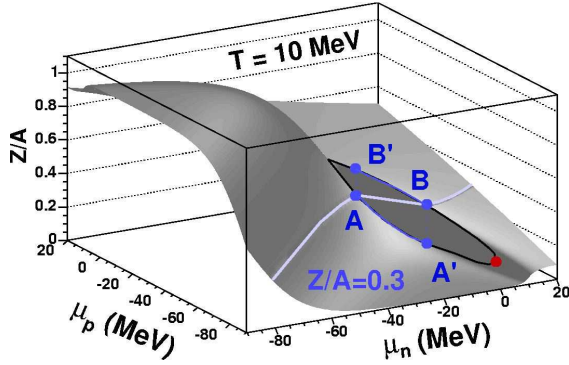


FIG. 9: $Z/A = \rho_p/(\rho_n + \rho_p)$ as a function of μ_n and μ_p for a fixed temperature $T = 10\text{ MeV}$. The path at $Z/A = 0.3$ is also shown.

curve with the corresponding constant- μ_n curve. Since the constant- μ_n curves are not aligned on constant- Z/A lines (except for symmetric matter), the constant- Z/A transformation does not make a transition from liquid to gas at a unique value of μ_n but shows a continuous smooth evolution of the intensive parameters along the coexistence line.

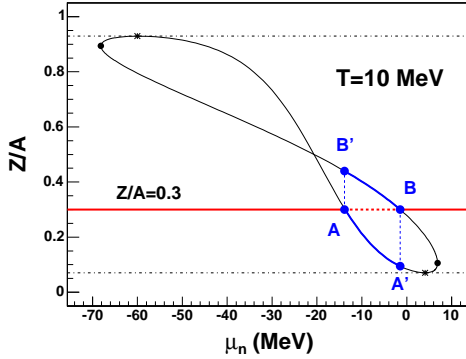


FIG. 10: Projection of the coexistence region in the Z/A versus μ_n plane. Black dots are critical points, and stars are points of maximal asymmetry. The path at $Z/A = 0.3$ is also shown.

The transformation $Z/A = 0.3$ is given as an example by the dotted lines in figure 8, and the grey path in figures 6,7,9. Let us follow this transformation from the low density phase. When the system reaches the coexistence border (point A), a liquid phase appears in B' at the same value of μ_n , μ_p and T . This point coincides with A in the representation of figure 6. We can see from figures 8 and 9 that the liquid fraction is closer to symmetric nuclear matter than the original system, as expected from the isospin-distillation phenomenon.

Following the system inside coexistence along the line $A - B$, the neutron chemical potential increases. Phase separation implies that, in this region, the system is com-

posed of two phases located at the coexistence boundaries and corresponding to the same value of the intensive parameters. The diluted phase goes along coexistence from A to A' while the dense phase goes on the other side of the coexistence border from B' to B. When it reaches B the gas is entirely transformed into a liquid, the phase transition is over and the $Z/A = 0.3$ transformation corresponds to a homogenous system again.

The evolution of μ_n during the transition can be quantitatively discussed on figure 10 which gives a projection of figure 9 on the μ_n axis. This figure clearly shows that a constant- Z/A transformation does not cross the coexistence at a unique μ_n value but explores a finite range of chemical potentials. The system is thus forced to follow the coexistence line in the intensive parameter space, as shown in figure 6 and in figure 11. The only exceptions are symmetric matter and the 2 maximum asymmetries of the coexistence region for each temperature.

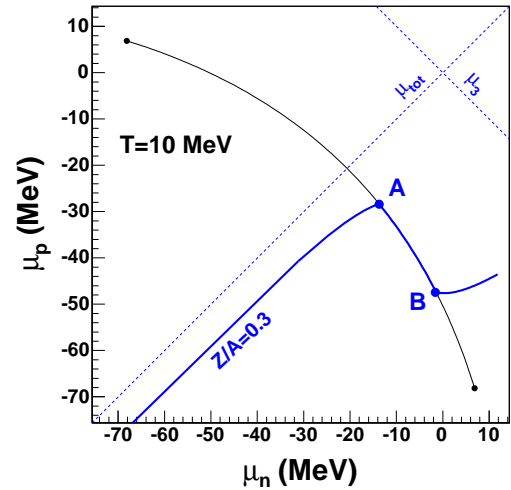


FIG. 11: Coexistence line, i.e. line of first-order phase transition, in the intensive-parameter plane (μ_n, μ_p) . The path at $Z/A = 0.3$ is also shown.

It is important to notice that the behavior shown in figures 10 and 11 is the generic behavior expected when a conservation law is imposed on an order parameter [22, 23]. Indeed, the usual discontinuity of the order parameter characteristic of a first-order transition is prevented by the constraint. If the system reaches coexistence, the only way to fulfill the conservation law on the order parameter is to follow the coexistence line until the conservation law becomes compatible with a homogeneous phase.

This continuous evolution by phase mixing hides the EOS discontinuity associated with the first-order phase transition. This is illustrated by the evolution of μ_n and P as a function of the total density ρ_{tot} at $Z/A = 0.3$ in figure 12. Full lines are obtained after the thermodynamic potential is made convex by phase mixing, i.e. with the Gibbs construction. These functions present no plateau

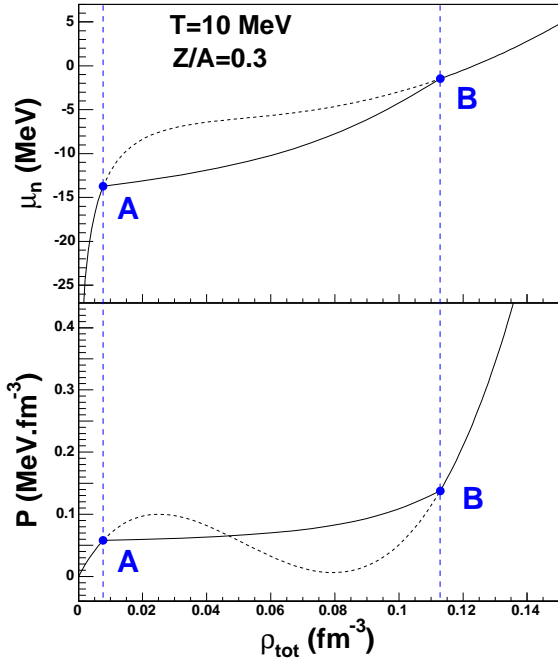


FIG. 12: Transformation at constant $Z/A = 0.3$ in nuclear matter at $T = 10 \text{ MeV}$. Top : $\mu_n(\rho_{\text{tot}})$. Bottom : $P(\rho_{\text{tot}})$. Dotted lines : solution for an homogeneous system. Full lines : Gibbs construction. Points A and B give the coexistence-region borders.

in the coexistence region, and the transformation looks like a continuous transition. Yet by definition the system is going through a first-order phase transition since the first derivatives of the grand potential are discontinuous.

This clearly stresses the fact that the behavior of specific transformations should not be confused with the intrinsic thermodynamic properties. Indeed a transformation is an explicit or implicit relation between the thermodynamic variables, e.g. a constant proton fraction Z/A implies $\rho_p = \rho_n Z/(A - Z)$. Then the variation of the intensive variables conjugated to one of the order parameters, e.g μ_n for ρ_n is given by :

$$\left(\frac{d\mu_n}{d\rho_n} \right)_{Z/A=cst} = \frac{\partial \mu_n}{\partial \rho_n} + \frac{\partial \mu_n}{\partial \rho_p} \frac{Z}{A - Z} \quad (35)$$

since

$$(\mu_n(\rho_n))_{Z/A=cst} = \frac{\partial f}{\partial \rho_n} \left(\rho_n, \rho_n \frac{Z}{A - Z} \right) \quad (36)$$

Then a first-order phase transition characterized by $\partial \mu_n / \partial \rho_n = 0$ leads to a continuous evolution of μ_n as a function of ρ_n according to eq.(35) because of the constraint of constant proton fraction.

The isospin degree of freedom does not change the order of the nuclear liquid-gas phase transition as claimed in different articles [7, 12]. It remains first order. Only

the constant-proton-fraction transformations (or other transformations constraining an order parameter) mimic a continuous transition because they do not cross the co-existence line at a single point, but are forced to follow it to fulfill the conservation law.

In general, transformations involving a constraint on an order parameter always appear continuous even in the presence of a first order phase transition [22, 23].

C. Phase diagram: $T = 0$ specificity

Until now we have presented a study at a fixed finite temperature. We will now consider the effect of temperature on the phase diagram, from the particular case of zero temperature to the symmetric-matter critical temperature T_c above which there is no transition any more.

The specificity of the zero-temperature case is the possibility to reach a vanishing density with a finite chemical potential [24], while at any finite temperature a given density can be zero only if the associated chemical potential goes to $-\infty$ (see eq.(17)). This is a trivial consequence of the specificity of Fermi-Dirac distribution at $T = 0$. In this case, the associated thermodynamic potential presents at zero density an edge with a finite slope, the associated finite chemical potential. An example is given by the (free) energy as a function of total density for symmetric nuclear matter in figure 1. Then, if the thermodynamic potential for the uniform system presents a concave region reaching zero density, the construction of the convex envelope does not reduce to the usual tangent construction between two points in coexistence. Indeed the interpolating plane defined by phase mixing will not be tangent to the thermodynamic potential on the zero-density edge.

The coexistence region at $T = 0$ is shown in figure 13. It can be divided into three zones corresponding to three kinds of equilibria with different conditions on the intensive parameters. In two small regions, labeled 2 in figure 13 and associated by isospin symmetry, both proton and neutron densities are finite in the gas phase. The usual bi-tangential construction can then be performed. This imposes the standard equality between all intensive parameters in the two phases A and B: $\beta(A) = \beta(B)$, $\mu_n(A) = \mu_n(B)$, $\mu_p(A) = \mu_p(B)$ and $P(A) = P(B)$. This region is limited on one side by a critical point beyond which there is no more curvature anomaly, and on the other side by the vanishing of one of the two densities in the gas phase. This second case corresponds to two symmetric regions denoted 1 in figure 13. There, we have equilibria for which the low density phase is on an edge $\rho_q = 0$, the second density being finite. For simplicity, let us take the case of globally neutron-rich matter where $\rho_p = 0$ and $\rho_n > 0$ at the low-density coexistence edge. In this case, the convex envelop is tangent to the thermodynamic potential of the uniform system only in the dense phase. This is a mono-tangential construction. It means that phase equilibrium does not require the equality of

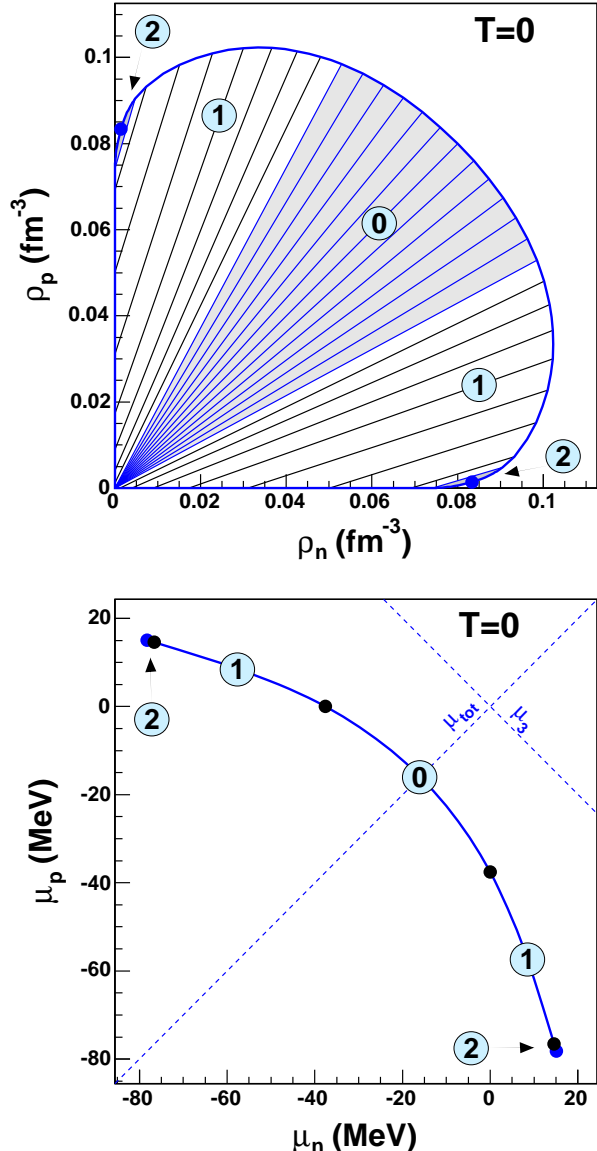


FIG. 13: Coexistence region at $T=0$. It is split into 3 different types of equilibria between liquid and gas (see text). Top : coexistence border (thick line) in the density plane. The straight lines relate two coexisting phases. Bottom : coexistence line in the plane of chemical potentials.

the potential derivative in the ρ_p direction, i.e. the equality of the proton chemical potentials in the two coexisting phases. Since the anomaly involves only the derivative in the ρ_p direction, the other equilibrium conditions characterizing the Gibbs construction are still satisfied in this region, namely the neutron chemical potential, pressure and temperature have to be the same in the two phases.

Since the construction involves two points with the same μ_n , we can use the neutron-grand-canonical proton-canonical potential G_{pC} (see section III-B) in order to reduce the problem to a one-dimensional case as illustrated in figure 14. This is a way to solve the problem in prac-

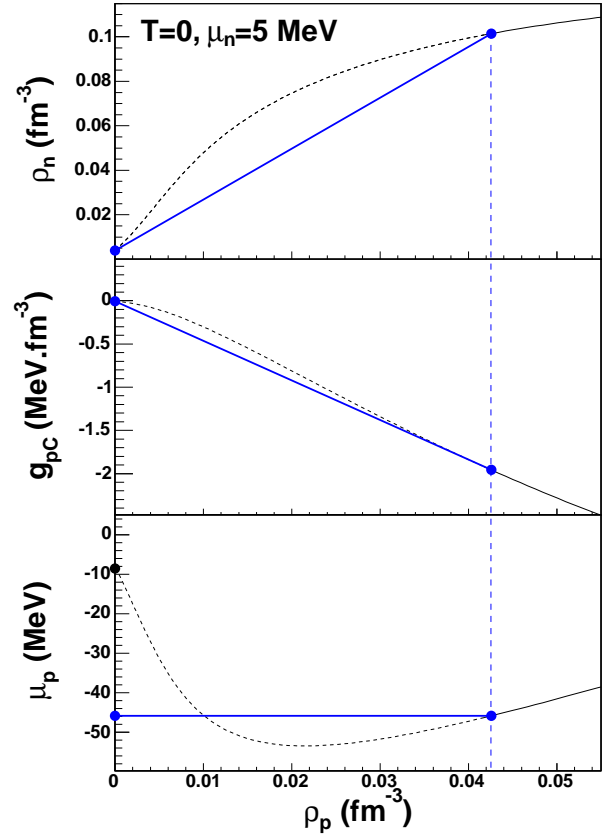


FIG. 14: Specificity of $T = 0$: Mono-tangential construction for a fixed neutron chemical potential $\mu_n = 5$ MeV. Upper part : corresponding path in the density plane. It reaches the edge $\rho_p = 0$ (with a finite ρ_n). Middle part: thermodynamic potential density g_{pC} (see section III-B). The concave region is corrected by phase mixing, which corresponds here to a mono-tangential construction (straight line). Lower part: μ_p . The mono-tangential construction on g_{pC} does not correspond to the usual Maxwell construction, that can not be performed because of the finite value of μ_p on the edge.

tice. Looking at a fixed μ_n for which the proton density reaches its edge $\rho_p = 0$ at zero temperature (upper part), we can see that a standard equal-area Maxwell construction is not possible in this case (lower part). However, the concave region in the thermodynamic potential (middle part) has to be corrected by phase mixing. Equilibrium is then given by a mono-tangential construction on g_{pC} .

Such equilibrium between a neutron gas and a two-fluid liquid leads to a discontinuous change of μ_p in the gas. Because of the dominance of region 1 with respect to region 2 in the phase diagram, the simplification is often made in the literature [24] that phase coexistence in neutron-star matter can be modeled as the equilibrium between neutron-rich nuclei and a pure neutron gas. It should however be noticed that this is possible only if the temperature is exactly zero, a finite proton fraction being associated to the gas phase at any finite temperature.

The last case, denoted 0 in figure 13, corresponds to

both $\rho_p = 0$ and $\rho_n = 0$ in the low-density phase. This case corresponds to a dense phase in equilibrium with the vacuum, i.e. at zero pressure. This region has a very simple physical interpretation. If the gas phase is given by the point $(\rho_n, \rho_p) = (0, 0)$, this means that the coexistence lines of zone 0 are constant Z/A lines. The coexistence border on the liquid side is the locus of zero pressure in the Z/A interval corresponding to region 0. For each value of Z/A , the liquid border is then given by the minimum of the energy per particle computed for this constant Z/A . Zone 0 corresponds then to the chemical potential interval in which a self-bound liquid can be defined.

D. Phase diagram: temperature dependence

In order to determine the phase diagram of nuclear matter, we establish the ensemble of points at equilibrium in the (ρ_n, ρ_p) plane for different fixed values of temperature. The result is represented in figure 15 as a function of the variables $(\rho, Z/A)$ in order to underline the role of isospin. Since protons and neutrons play symmetric roles, the resulting curves are symmetric with respect to the axis $Z/A = 0.5$. For this reason, in the following, only the neutron-rich part ($Z/A < 0.5$) will be discussed.

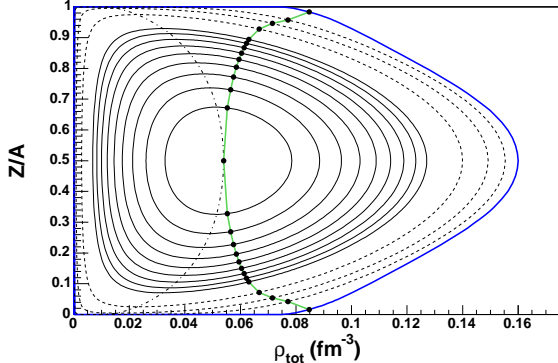


FIG. 15: Coexistence region in the $(\rho, Z/A)$ plane at different temperatures. Thick line : $T = 0$. Dotted lines : $T = 4, 6, 8 \text{ MeV}$. Solid lines : $T = 10, 10.5, 11, 11.5, 12, 12.5, 13, 13.5, 14 \text{ MeV}$. Black dots : critical points at each temperature, including $T_c = 14.54 \text{ MeV}$. Dashed-dotted line : points of maximum asymmetry for coexistence at each temperature.

The widest coexistence region corresponds to zero temperature. Equilibrium points that belong to the edge $\rho_p = 0$ make a line at $Z/A = 0$. When temperature is introduced, coexistence region concerns non-zero values of ρ and Z/A , which means that equilibrium is always between phases containing both kinds of particles.

The critical points are also reported for each temperature. They are second-order-transition points. They form a critical line. An interesting feature is that the

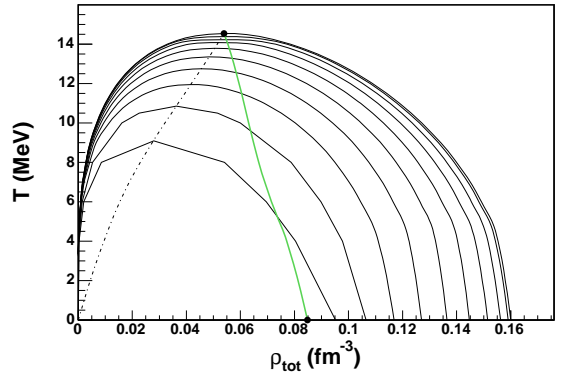


FIG. 16: Cuts of the coexistence region as a function of the total density for regularly spaced values of Z/A between 0.05 and 0.5. Thick grey line : line of critical points. Dashed-dotted line : line of maximum asymmetry.

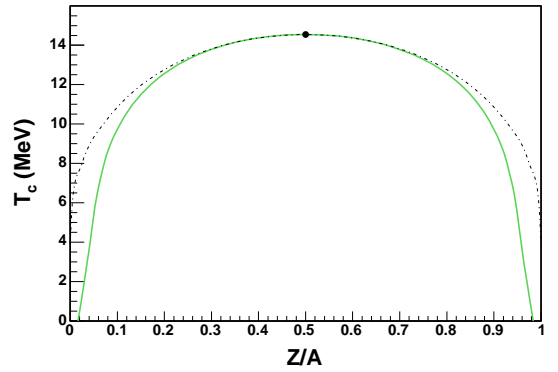


FIG. 17: Critical temperatures as a function of the system Z/A (thick grey line). The curve of maximal temperatures for coexistence is also shown (dashed-dotted line).

critical density increases with the asymmetry while the critical temperature decreases, as can also be seen from figures 16 and 17. This is in agreement with previous studies using different effective interactions [7, 21].

It should be stressed that, on each coexistence curve at a fixed temperature, the critical points do not correspond to the minimum (or maximum) Z/A . This point $((Z/A)^{min}, \rho^{min})$ is situated at a density lower than the critical point, i.e. on the gas side of coexistence. As a result, transformations can be performed at constant Z/A such that the system enters at a point of coexistence as a gas and exits at another point still as a gas. This is the so-called retrograde transition [1]. This happens for the small region for which $(Z/A)^{min} < Z/A < Z/A^c$. Between those two points, there is appearance and disappearance of a liquid phase at $(Z/A)^L > Z/A$ at equilibrium with a gas at $(Z/A)^G < Z/A$. For a too neutron-rich system such that $Z/A < (Z/A)^{min}$, there can be no phase coexistence.

As temperature grows, the coexistence region is reduced. The values of $(Z/A)^c$ and $(Z/A)^{min}$ become closer to the symmetry $Z/A = 0.5$. Densities ρ^c and ρ^{min} follow opposite evolutions: ρ^{min} grows with temperature, while ρ^c diminishes. The coexistence region disappears at the critical temperature T^c , for which only symmetric matter presents a second-order transition point. Critical and minimum Z/A lines join at this ultimate critical point.

It is also interesting to look at the coexistence zone as a function of Z/A (see figures 16, 17). We can see that the dependence of the critical temperature (as well as the maximal temperature) on Z/A is weak. Only for very high values of asymmetry the difference between the two temperatures for a fixed Z/A can be several MeV. This is another way to visualize the retrograde transition, meaning that we can have saturated vapor at supercritical temperatures.

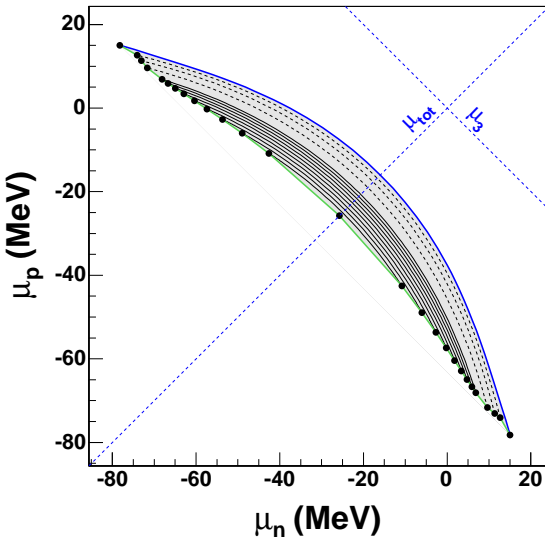


FIG. 18: Phase diagram in (μ_n, μ_p) for different values of T . Thick line : $T = 0$. Dotted lines : $T = 4, 6, 8$ MeV. Solid lines : $T = 10, 10.5, 11, 11.5, 12, 12.5, 13, 13.5, 14$ MeV. Black dots : critical points at each temperature, including $T_c = 14.54$ MeV.

Finally, it is interesting to look at the coexistence manifold in the (β, μ_n, μ_p) space, as shown in figure 18. One can see that the coexistence is almost perpendicular to the $\mu_3 = 0$ axis, stressing the fact that the nuclear liquid-gas phase transition is dominated by its isoscalar component [25, 26].

E. Critical behavior

Let us now study in more details the critical behavior of the system. Conversely to the usual single-fluid liquid-gas phase transition which presents a unique critical point, a two-fluid system is critical along a line in

the (β, μ_n, μ_p) intensive-parameter space. The critical points are obtained for each temperature (below the symmetric-matter critical temperature) by determining the μ_n value for which the two phases with the same tangent plane merge together. To evaluate this point, we have used both the Maxwell construction in the neutron-grand-canonical proton-canonical ensemble (see section III-B) and the existence of a crossing point in the P versus μ_p curve at constant (T, μ_n) . The critical points also correspond to the disappearance of a concave region in the uniform-system free energy. This disappearance of the spinodal region provides an independent way to evaluate the location of the critical line: we can represent as a function of μ_n the lower value of the free-energy curvature in the (ρ_n, ρ_p) plane. The resulting curve crosses the horizontal axis at the critical value of μ_n . Below the symmetric-matter critical point T_c , these methods lead to the definition of two symmetric critical lines, one for neutron-rich systems ($\mu_n = \mu_n^>(T), \mu_p = \mu_p^<(T)$) and the other for the opposite isospin ($\mu_p = \mu_p^>(T), \mu_n = \mu_n^<(T)$).

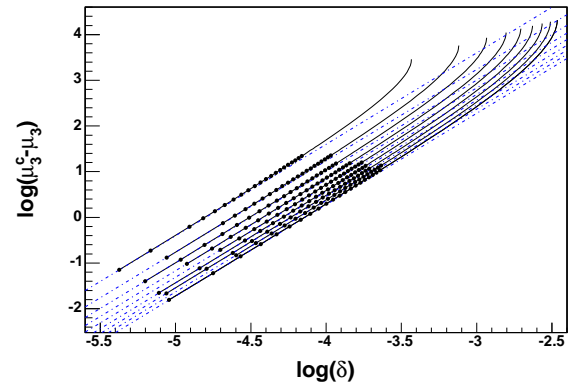


FIG. 19: Solid lines with points : evolution of $\mu_3^c - \mu_3$ as a function of δ (see text) near the critical point for different temperatures : $T = 10, 10.5, 11, 11.5, 12, 12.5, 13, 13.5, 14$ MeV. Straight dashed-dotted lines : power laws with critical exponent $\beta_\beta = 2$.

At the approach of the critical point, the distance in the space of observables between the two phases (A and B) in equilibrium, i.e. the order parameter, goes to zero as a power of the distance to the critical point in the intensive-variable space. The resulting power law is characterized by the critical exponent β . In order to study this behavior for nuclear matter in the (ρ_n, ρ_p) plane, we consider a distance $\delta = \sqrt{(\rho_n^B - \rho_n^A)^2 + (\rho_p^B - \rho_p^A)^2}$. In a two-fluid system the behavior of this distance can be studied in two ways.

First, for a fixed temperature $T = \beta^{-1}$, δ is expected to depend on the chemical potentials as :

$$\delta_\beta(\mu_q) \propto (\mu_q^c - \mu_q^q)^{1/\beta_\beta} \quad (37)$$

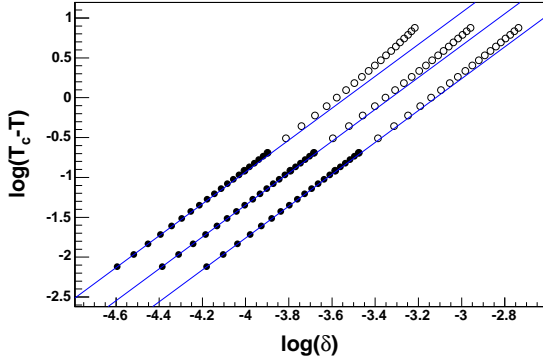


FIG. 20: Points : evolution of $T - T_c$ as a function of δ (see text) near the critical point for different μ_n : $\mu_n = \mu_q^<(T_c)$, $\mu_q^<(T = 12\text{MeV})$, $\mu_q^<(T = 10\text{MeV})$. Straight lines: power laws with critical exponent $\beta_{\mu_n} = 2$.

where β_β is the critical exponent at a fixed temperature and μ_q^c the critical value of μ_q for the considered temperature. Since μ_n and μ_p are constrained to be on the coexistence line, the above relation is independent of the chemical potential selected to perform the study. For symmetry reasons we have introduced the isoscalar $\mu = \mu_n + \mu_p$ and the isovector $\mu_3 = \mu_n - \mu_p$ chemical potentials. Since the dependence on μ is negligible (see figure 18), we have focused our study on the evolution of δ with μ_3 . The results are presented in figure 19. We can observe that our results perfectly follow the expected critical behavior with the mean-field value $\beta_\beta = 2$.

For a fixed value of μ_q , the distance δ_{μ_q} goes to zero as the temperature tends to the critical one β^c . The power law should be :

$$\delta_{\mu_q}(\beta) \propto (\beta^c - \beta^q)^{1/\beta_{\mu_q}} \quad (38)$$

where β_{μ_q} is the critical exponent at a fixed μ_q . Again, since the temperature β and the chemical potential μ_q in coexistence are related by a Clapeyron-like relation, the above study leads to the same critical behavior if studied as a function of $\mu_{q'}$ with $q' \neq q$, instead of β . In figure 20 we present the evolution with temperature for different chemical potentials. This graph shows that our results fulfill the mean-field scaling $\beta_{\mu_q} = 2$.

V. CONCLUSION

In this paper, based on a mean-field analysis of nuclear matter with a realistic Skyrme SLy230a effective interaction,

we have established that nuclear matter presents a first-order phase transition even when the isospin degree of freedom is explicitly accounted for. This results from the existence of a spinodal region, which is a region where the free energy of a homogeneous system is concave. In the case of infinite systems, such curvature anomaly is corrected by constructing the convex envelope. This is a tangent construction that links pairs of points in the space of observables with the same values for the intensive parameters. It corresponds to points of discontinuous first derivatives for the grand-canonical potential of the system in the space of Lagrange intensive parameters, along a coexistence manifold limited by a critical line. Except on this limit which corresponds to a second-order phase transition, the slope discontinuity demonstrates that the system is undergoing a first-order phase transition. For fixed values of temperature (below the symmetric-matter critical one), coexistence lines are obtained in the chemical-potential plane. They are limited by critical points that correspond to proton fractions depending on the temperature. As lower temperatures are considered, more asymmetric nuclear matter can be involved in a first-order phase transition.

As for the study of critical behaviors, we have found that all the numerical data can be fitted by power laws with critical exponents equal to 2, which is consistent with generic mean field predictions [27]. Calculations beyond mean field are needed to obtain a result which could be characteristic of a given universality class. Looking at the isospin content of the phases, we show that the proton fraction is discontinuous at the phase transition except at the critical points and for symmetric matter. In asymmetric nuclear matter, the proton fraction can be used as an order parameter. When the transition occurs, the liquid gets closer to symmetry while the gas is enriched in the more abundant species. This is the well-known isospin fractionation. This has a strong influence on the constant-proton-fraction transformations, since in order to fulfill the imposed conservation on an order parameter, the transformation is forced to follow the coexistence line instead of crossing it. This hides the slope discontinuity characteristic of a first-order phase transition, the transformation appearing as continuous.

- [5] J.M.Lattimer and M.Prakash, Phys. Rep. 333 (2000) 121
- [6] N.K.Glendenning, Phys. Rep. 342 (2001) 393.
- [7] H.Muller and B.Serot, Phys. Rev. C52 (1995) 2072.
- [8] C.B.Das et al, Phys. Rev. C67 (2003) 064607;
- [9] W.L.Qian, S.R.Keng, Journ. Phys. G (2003) 1023
- [10] T.Sil et al., Phys. Rev. C69 (2004) 14602
- [11] B.K.Srivastava et al., Phys. Rev. C65 (2002) 054617
- [12] J.M.Carmona et al., Nucl. Phys. A643 (1998) 115
- [13] E.Chabanat et al., Nuclear Physics A627 (1997) 710-746.
- [14] R. Balian, From Microphysics to Macrophysics, Springer Verlag, 1982.
- [15] M.Barranco, J.R.Buchler, Phys. Rev. C24 (1981) 1191
- [16] J.M.Lattimer, C.J.Pethick, D.G.Ravenhall, D.Q.Lamb, Nucl. Phys. A432 (1985) 646
- [17] S.Schlomo, V.M.Kolomietz, Rep. Prog. Phys. 68 (2005) 1
- [18] F.Douchin, P.Haensel and J.Meyer, Nucl. Phys. A665 (2000) 419
- [19] D.Vautherin, Adv. Nucl. Phys. 22 (1996) 123.
- [20] V.Baran et al, Nucl.Phys. A632 (1998) 287.
- [21] B.A.Li, C.M.Ko and W.Bauer, Int. Journ. Mod. Phys. E7 (1998) 147
- [22] Ph.Chomaz and F.Gulminelli, in 'Dynamics and Thermodynamics of systems with long range interactions', Lecture Notes in Physics vol.602, Springer (2002)
- [23] F. Gulminelli et al, Phys.Rev.E68 (2003) 026120.
- [24] C.J.Pethick, D.G.Ravenhall, C.P.Lorenz, Nucl. Phys. A584 (1995) 675.
- [25] J.Margueron, Ph. Chomaz, Phys. Rev. C67 (2003) 041602;
- [26] V.Baran et al, Phys. Rep. 410 (2005)335.
- [27] H.E.Stanley, Introduction to phase transitions and critical phenomena, Oxford University press, 1971.
- [28] Phase transitions are related to the properties of the thermodynamic potential partial derivatives with respect to thermodynamic variables (i.e. extensive observables x_i and their intensive conjugates y_j). A transformation is defined by a given path ($x_i = f_i(\lambda)$, $y_j = g_j(\lambda)$), where λ is a curvilinear coordinate. The thermodynamic potential total derivative for this transformation is :

$$\frac{dG}{d\lambda} = \sum_i \frac{\partial G}{\partial x_i} f'_i + \sum_j \frac{\partial G}{\partial y_j} g'_j$$

The properties of this total derivative depend on the specific path, while the transition is characterized by the partial derivatives alone.